18.086 Final Project: Finite Element Modelling of Ionic Liquid Flow Through Porous Electrospray Emitters

Robert S. Legge Jr.*
*Massachusetts Institute of Technology/Department of Aeronautics and Astronautics, Boston, USA

***Abstract*—A numerical simulation based on finite differences was created to model fluid flow through the bulk of a porous metal electrospray emitter. The model calculates the maximum fluid flow, and corresponding ionic current, for a given pressure head at the emitter tip. Numerical results are given for variations in: emitter geometry, electric field strength at the emitter tip, fluid properties, and finally pore diameter and the introduction of porosity gradients of differing shapes.**

I. Introduction

Traditional colloid thrusters utilize pressure fed capillary emitter geometry to transport liquid to the tips of emitter structures, where Taylor cones are formed. This requires pressurization systems on-board the spacecraft which add both mass and complexity. The difficulties in fabricating small, uniform capillaries also pose problems in terms of miniaturization of needle arrays. One way to avoid these issues is to use externally wetted emitter geometries where the liquid is drawn from its reservoir by capillary forces alone. Such passively fed systems supply liquid at the rate established by the electrospray emission process. The use of externally fed emitters in vacuum is possible with ionic liquids such as EMI-BF_4[1], [2], [3]. These liquids are molten salts at room temperature and exhibit extremely low vapor pressures making them ideal for use in vacuum. They are formed by positive and negative ions which both can be directly extracted and accelerated to produce thrust when used in bipolar operation[4].

A. Porous Metal Emitters

A simple capillary electrospray emitter setup is shown in Figure 1. An applied potential between an extractor electrode and conductive liquid inside a capillary causes a liquid meniscus at the end of the capillary to deform into a conical shape. This structure is called a taylor cone in honor of G.I. Taylor who first derived a mathematical model to describe the phenomenon in 1964[5] for certain conditions. The apex of the cone emits a jet of charged liquid which breaks up into charged droplets. These droplets are then accelerated by means of an electrostatic force to a final exit velocity. In thruster applications, the electrostatic force applied to the charged droplets is equal but opposite to the resulting thrust felt by the thruster device. In cases where the local electric field at the tip of the taylor cone is high enough, the electrostatic pull overcomes the ion surface energy and ions are extracted directly from the liquid. This causes the ions to be accelerated through the potential and achieve a much higher exit velocity, which is a more efficient propulsion system in terms of propellant consumption, albeit at the expense of lower thrust.

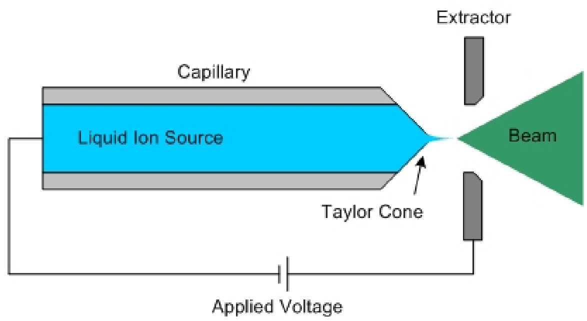

Fig. 1. Capillary Electrospray Emitter Setup

B. Importance of Fluid Flow on Emitter Operation

Since the amount of thrust of an electrospray emitter is rate limited by the number of ionic liquid ions that are able to reach the emission region, the physics behind fluid flow might greatly effect overall performance. The fluid transport in porous metal electrospray emitters is entirely passive which places even more importance on accurate flow models. In this paper, a first pass attempt will be made to characterize the maximum amount of current that can be extracted from a porous emitter in steady state operation. The paper is presented as follows: first the numerical modelling is explained and various discretization derivations are presented. Next, flow results are shown for a number of variational parameters including emitter substrate properties, ionic liquid properties and the the effect of emitter size and the addition of a porosity gradient. Finally, conclusions are drawn as to what the results mean for the operation of electrospray emitters.

II. Problem Setup

The numerical scheme will implement a finite difference simulation of the two-dimensional flow equation (Equation 1) using Darcy's Law. The simulation will be solved in two dimensions and will assume axial symmetry for the emitter. Inputs for the model will be a pressure head dirichlet boundary condition on the emitter tip as well as various geometrical constants which detail the emitter porosity as well as fluid properties.

$$\frac{\partial}{\partial x}\left(K_x\left(x\right)\frac{\partial}{\partial x}\left(h\right)\right)+\frac{\partial}{\partial y}\left(K_y\left(x\right)\frac{\partial}{\partial y}\left(h\right)\right)=0 \tag{1}$$

Where K_x and K_y are the effective fluid conductivity of the liquid in the porous media. For this application, K will only vary with x so that in the second term, it can be considered a constant and taken out of the expression.

A. *Darcy's Law and the Effective Fluid Conductivity*

The fluid conductivity for the system is dependant on both parameters of the porous media, but also of some parameters which characterize the fluid properties. The general relation which explains why K is a conductivity is given below:

$$\hat{q} = K \nabla h \tag{2}$$

Which states that the flow rate per unit area is equal to the conductivity times the hydraulic potential gradient. The general analytical expression for finding the value of the conductivity is given as:

$$K = \frac{\kappa \rho g}{\mu} \tag{3}$$

Where κ is the intrinsic permeability of the porous substrate, ρ is the density of the fluid, g is the gravitational constant at sea level, and μ is the dynamic viscosity of the fluid.

The intrinsic permeability of the porous media depends on many factors including the average pore diameter, the complexity of flow channels, the relative reynolds number of the flow, and etc... It is a quantity that is best found experimentally, although some analytical solutions exist. One analytical model for the fluid conductivity is given by the Kozeny-Carman equation of the following form[6]:

$$K = \frac{\rho g}{\mu}\kappa = \frac{\rho g}{\mu}\frac{d^2\phi^3}{180\left(1-\phi\right)^2} \tag{4}$$

Where ϕ is the total porosity and d is the representive particle diameter. Of course, for our application, we only know the pore size and would need a way to connect the pore size to the effective particle diameter. Figure 2 shows the fluid conductivity plotted as a function of particle diameter assuming a total porosity of 0.75, which has been experimentally found for our samples.

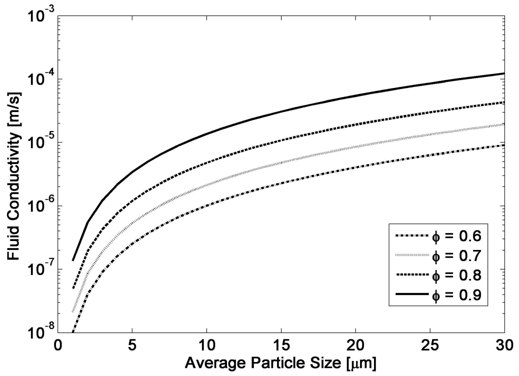

Fig. 2. Fluid Conductivity given as a function of Pore Diameter for the Kozeny-Carman Equation

A better way to find the effective fluid conductivity is to use experimental data. Data provided by Mott Corporation, a porous metal supplier, was used to generate an analytical approximation for the intrinsic permeability as a function of both dynamic viscosity and average pore diameter. The predictions of the model were based on curve fits to the experimental data provided and are:

$$\kappa = 1.9734 \times 10^{-13}\left(\mu\right)^{-2.0021}\left(D_P\right)^{1.2542} \tag{5}$$

Where D_P is the average pore diameter in μm. Figure 3 shows the model predictions (solid lines) and the corresponding experimental values. The model provides a rough estimate for the intrinsic permeability that will be utilized in the finite difference scheme.

B. *Descritizing Darcy's Law*

The dicretization scheme used is a standard central difference scheme in the non varying porosity direction and a central difference scheme using a

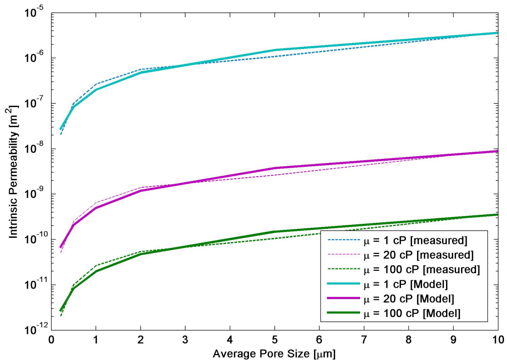

Fig. 3. Intrinsic Permeability vs Pore Size and Viscosity as: predicted by the model (solid) and given by experimental data (dotted)

staggered grid to approximate the porosity gradient in the directions of varying porosity. The flow equation can be re-written as:

$$0 = \frac{\partial}{\partial x} \left(K \left(x \right) U_x \right) + K \left(x \right) U_{yy} \tag{6}$$

The term in the y direction is trivial, and as was said before, will be approximated using the following central difference scheme:

$$U_{yy} = \frac{U_{i,j+1} + 2U_{i,j} + U_{i,j-1}}{\left(\Delta y \right)^2} \tag{7}$$

The term in the x direction is a little more complicated. If we say that:

$$V = K \left(x \right) U_x = K_{i+\frac{1}{2},j} \left(\frac{U_{i+1,j} - U_{i,j}}{\Delta x} \right) \tag{8}$$

And then the derivative of this expression in the x direction is approximated by:

$$V^{'} = \frac{V_{i,j} - V_{i-1,j}}{\Delta x} \tag{9}$$

$$V^{'} = \frac{K^{+} U_{i+1,j} - \left(K^{+} - K^{-} \right) U_{i,j} + K^{-} U_{i-1,j}}{\left(\Delta x \right)^2} \tag{10}$$

Where $K^{+} = K_{i+\frac{1}{2}}$ and $K^{-} = K_{i-\frac{1}{2}}$. Figure 4 shows a graphical description of the stencil used in the above numerical approximation.

C. Simulation Geometry and Boundary Conditions

In order to model the emitter geometry effectively, the geometry to be modeled is a triangular region shown in Figure 5. The right side, as well as the flat top piece, are modelled with homogeneous dirichlet boundary conditions to model the constant head of the fluid reservior. This sets the zero head reference point corresponding to atmospheric pressure conditions. The left side is modelled with a heterogenous dirichlet boundary that serves to set the electrostatic traction pressure, which drives the flow. The diagonal side of the emitter as well as the bottom are modelled as neumann conditions with zero-flow. The bottom is an axi-symmetric line if we assume that the emitter is a cone.

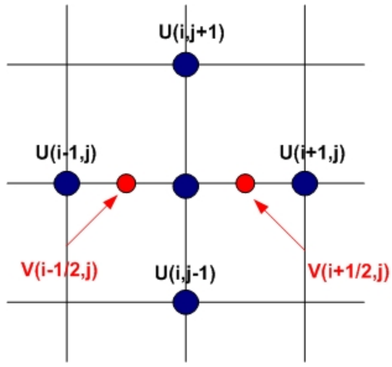

Fig. 4. Numerical stencil used to model flow

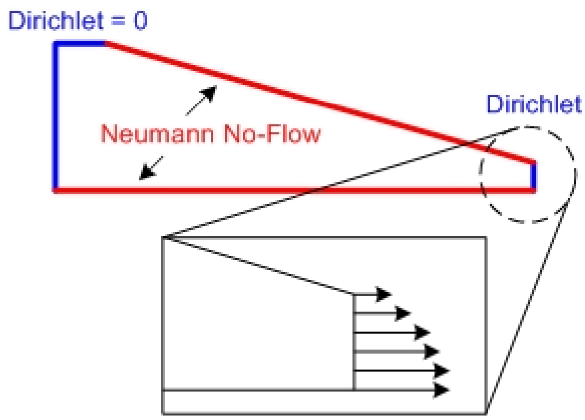

Fig. 5. Geometry used in numerical scheme

The numerical descretization was acheived by using a modified version of the MatLab numgrid function. Simulations were carried out using three geometries with different dimensions corresponding to those shown in Figure 6. The important geometric parameters include: the overall emitter length (L), the emitter width (w), the tip diameter (d), and the emitter cone half angle (α). Table I shows the geometry that was tested. The parameters that were varied were L and W while d and α were kept constant.

D. Run Parameters

Current flow results will be obtained as a function of the applied voltage between the extractor electrode and the emitters. This voltage will be linked

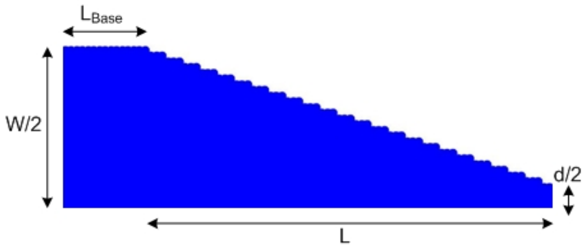

Fig. 6. Geometrical Measurements

Sample #	L $[\mu m]$	W $[\mu m]$	d $[\mu m]$	θ [deg]
1	839	593	15	19.5
2	622	445	15	19.7
3	395	297	15	20.5

TABLE I
EMITTER GEOMETRY

to a pressure head at the emitter tip through an electrostatic model. The head will consist of the difference between the enhanced electric field at the emitter tip and the electric field required to overcome surface tension and produce flow from the tip. The excess pressure will be the driving pressure for the flow through the bulk material. The excess electric field can be written as:

$$\Delta P = \frac{1}{2}\epsilon_0 E_{tip}^2 - \frac{2\gamma}{\bar{r_c}} \tag{11}$$

Where γ is the surface tension of the fluid and $\bar{r_c}$ is the average radius of curvature of the emitter tip. The pressure head can be then written as:

$$h = \frac{\Delta P}{\rho g} \tag{12}$$

Results will be obtained for: the three different emitter geometries and four different liquids as well as three different porosity configurations. The ionic liquids to be tested each have different physical properties (e.g. density and viscosity) that will affect performance. Table II shows the properties of the four liquids. In addition, three different porosity configurations will be tested, including: a constant porosity with a pore diameter of $0.5\mu m$, an 5:1 linear porosity gradient with $2.5 mum$ at the base and $0.5\mu m$ at the emitter tip, and a 5:1 non-linear porosity gradient with $2.5 mum$ at the base and $0.5\mu m$ at the emitter tip. The porosity gradients are plotted in Figure 7.

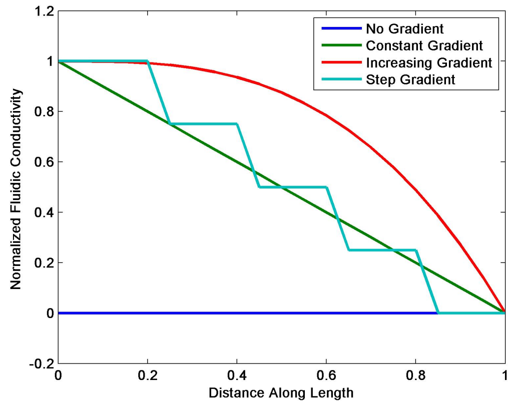

Fig. 7. Different Porosity Functions

Ionic Liquid #	Density $[kg\,m^{-3}]$	Viscosity $[cP]$
EMI-BF_4	1271	37
EMI-IM	1517	41
C_5MI-$(C_2F_5)3PF_3$	1600	61
EMI-$(CF_5SO_2)_2N$	1590	140

TABLE II
IONIC LIQUID PROPERTIES

III. DATA PROCESSING

The numerical simulation solved for the pressure head in the porous emitter. In order to solve for the flowrate at the emitter tip, the following equation must be used:

$$\hat{q} = K\frac{\partial h}{\partial x} \tag{13}$$

Where we obtain the pressure gradient at the tip through the following approximate formula:

$$\frac{\partial h}{\partial x} \approx \frac{h_{i(tip)-1,j} - h_{i(tip),j}}{\Delta x} \tag{14}$$

This gives the flowrate per unit area passing through the emitter tip as:

$$\hat{q} = K\frac{\partial h}{\partial x} \tag{15}$$

And then the actual flowrate passing through the emitter tip is then:

$$q = \hat{q}\pi\left(r_c\right)^2 \tag{16}$$

By knowing the limiting flowrate, we can then solve for the maximum current that can be emitted from the emitter tip, as this is what ultimately effects performance in our application. The relationship between current and liquid flowrate is given as:

$$I = q\rho\left(\frac{\bar{q}}{m}\right) \quad (17)$$

Where ρ is the fluid density and $\frac{\bar{q}}{m}$ is the average charge to mass ratio of the emitted ions, which for this analysis will be set at 440000 C/kg which corresponds to the liquid EMI-BF_4 operating in the positive polarity. In a more detailed analysis, the charge to mass ratios for the different ionic liquids would have to be experimentally found.

IV. Results and Discussion

A. Effect of Increasing Pore Size

As the average pore diameter d is increased, we would expect that the amount of emitted current would increase due to an increase in the hydraulic conductivity. Figure 8 shows results from the numerical model. Shown is the maximum current plotted as a function of emitter tip electric field for various values of average pore diameter. We see that as the electric field increases, the current increases. A more interesting result is that as the average pore size increases, the amount of current that increases per unit increase in electric field increases.

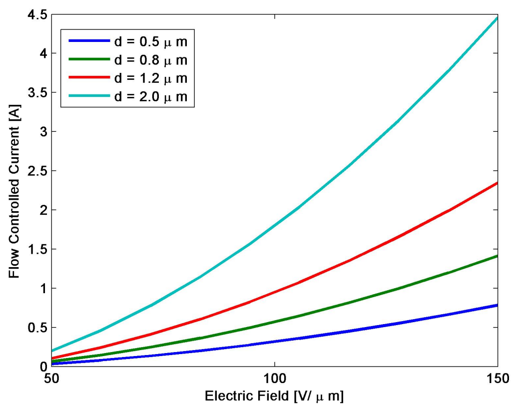

Fig. 8. Current vs. Electric Field for Different Average Pore Sizes

B. Effect of a Porosity Gradient

One way that has been postulated to increase the fluid flow to the emitter tip would be to introduce a porosity gradient to actively pump fluid to the emitter tip. Figure 9 shows a resulting pressure head profile along the length of the emitter for the different porosity gradient configurations. Since the amount current that can be extracted is directly proportional to the slope of the head at the emitter tip, we want the pressure drop to be largest here. In terms of this criterion, we would expect that the most current would be produced by the non-linear gradient case, and the least to be produced by the constant porosity case.

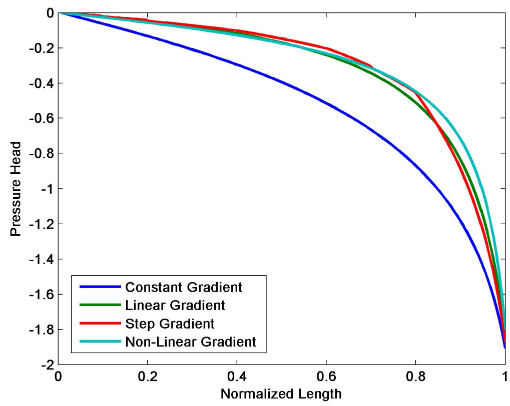

Fig. 9. Pressure Head as a Function of Emitter Length for Different Porosity Gradients

Figure 10 shows the emitted current as a function of average pore diameter at the emitter tip for the four porosity configurations. We see that as expected, the non-linear porosity gradient has the largest emitted current while the constant porosity case has the least. We see that by introducing a porosity gradient we can significantly increase the maximum emitted current, while at the same time, we can make sure that the fluid preferentially travels to the emitter tip.

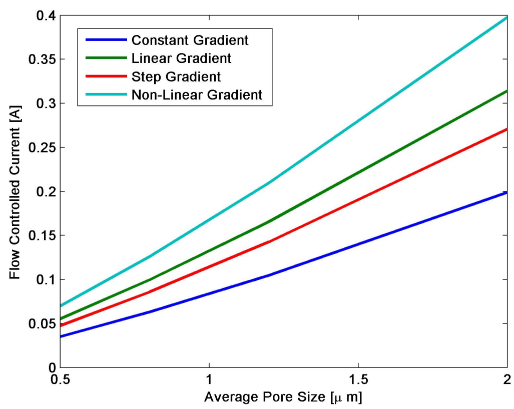

Fig. 10. Current vs. Pore Size for Different Porosity Gradients

C. Effect of a Emitter Size

Another aspect of electrospray emitters that can be modelled using this technique is what happens as the whole emitter is miniaturized. On first pass, it is obvious that as the emitter's size is reduced, and its tip geometry and aspect ratio remain constant, that the amount of current that can be extracted should increase, since the fluid has less distance to travel through the porous emitter material. Figure 11 shows the results of the numerical simulation for emitters of three different sizes. We see that as the emitter size is reduced, the maximum amount of emitted current increases significantly. Figure 12 shows the maximum amount of current plotted as a function of emitter porosity at the tip, which also shows the same trend.

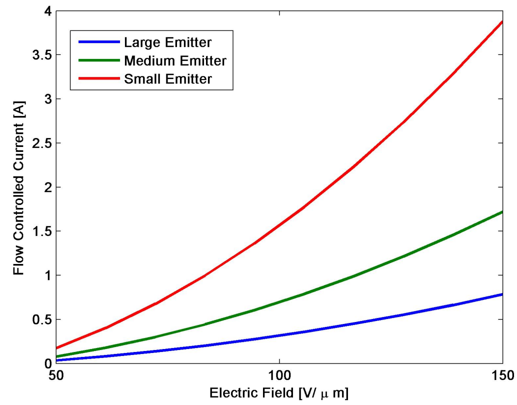

Fig. 11. Current vs. Tip Electric Field for Emitters of Different Sizes

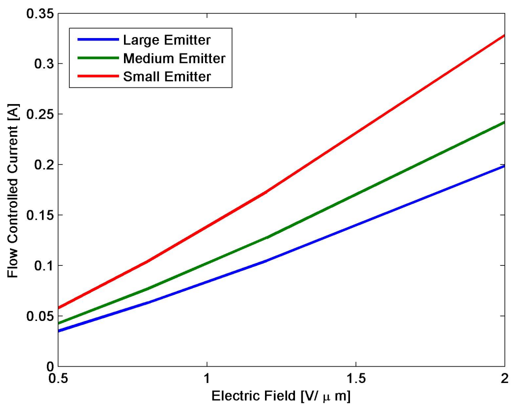

Fig. 12. Current vs. Pore Size for Emitters of Different Sizes

D. *Effect of Different Ionic Liquids*

One final variation that was calculated was how liquids with different physical properties affect the maximum emitted current. Four liquids were run with the simulation and we see, in Figure 13, that the different liquids have a large effect on fluid transport through the emitters. The results are primarity a function of the liquid's viscosity and surface tension, and that EMI-IM will emit the most current.

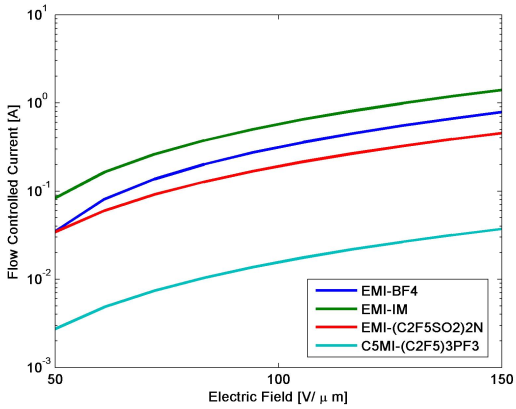

Fig. 13. Current vs. Pore Size for Different Ionic Liquids

V. Conclusions

The results of this project have shown that the flow of ionic liquids through the porous emitters is not the limiting factor in the magnitude of the emitted current. Additionally, the model can be used in the future to explore better emitter geometries, for increasing or decreasing the amount of emitted current for a particular application. The model will also be useful in the future to explore how emitters in an array will impact each other in terms of performance, and what the resulting flow nets look like. Lastly, the code could also be implemented to explore the effects of pore blocking and clogging on performance.

References

[1] I. Romero-Sanz and R. Bocanegra and M. Gamero-Castaño and J. Fernandez de la Mora, "Source of Heavy Molecular Ions Based on Taylor Cones of Ionic Liquids Operating in the Pure Ion Evaporation Regime," *Journal of Applied Physics*, vol. 94, No. 94, pp. 3599-3601, 2003.

[2] Paulo Lozano and Manuel Martinez-Sanchez, "Ionic Liquid Ion Sources: characterization of externally wetted emitters," *Journal of Colloid and Interface Science*, No. 282, pp. 415-421, 2005.

[3] Robert S. Legge, Paulo C. Lozano and Manuel Martinez-Sanchez, "Fabrication and Characterization of Porous Metal Emitters for Electrospray Thrusters," 30^{th} *International Electric Propulsion Conference*, No. 145, 2007.

[4] Paulo Lozano and Manuel Martinez-Sanchez, "Ionic Liquid Ion Sources: Suppression of Electrochemical Reactions Using Voltage Alternation," *Journal of Colloid and Interface Science*, No. 280, pp. 149-154, 2004.

[5] G.I. Taylor, "Disintegration of Water Drops in an Electric Field," *Proceedings of the Royal Society of London*, Vol. 280, pp. 383-397, 1964.

[6] Charles Harvey, "MIT 1.72 Groundwater Hydrology Class Lecture Notes,"